Assessment of the GraphCast AI model for precipitation forecasting and its potential in extreme event prediction over Bangladesh

Munad Hasan[1], Shabista Yildiz[2*] & Mohammad Kamruzzaman[3]

[1]Department of Meteorology, Faculty of Earth and Environmental Sciences, University of Dhaka, Dhaka, Bangladesh, Email: munad-1-2020017017@met.du.ac.bd

[2]Department of Meteorology, Faculty of Earth and Environmental Sciences, University of Dhaka, Dhaka, Bangladesh, Email: shabistayildiz@du.ac.bd; ORCID ID: 0009-0007-4131-5542

[3]Farm Machinery and Postharvest Technology Division, Bangladesh Rice Research Institute, Gazipur, Bangladesh; Email: milonbrri@gmail.com; ORCID: 0000-0001-6640-8082

[*]Corresponding Author: shabistayildiz@du.ac.bd
Shabista Yildiz

Abstract

Bangladesh situated in the tropical monsoon region is one of the most rainfall-sensitive countries in the world with terrain ranging from northwest floodplains to southern coastal deltas to eastern hilly regions. This complex landscape coupled with intensified climate variability influences local convection and extreme precipitation events, making short range forecasting particularly difficult. In this context, AI driven weather forecasting is gaining promise in diagnosing nonlinear atmospheric processes where conventional physics-based models fall short. Therefore, this study employs AI-based GraphCast model to forecast 1-, 2-, and 3-day cumulative rainfall over Bangladesh utilizing observational data from 43 Bangladesh Meteorological Department (BMD) stations during 2023-2024. Then, the performance of the model has been evaluated against global forecasting models namely ECMWF and GFS with statistical metrics including correlation coefficient (CC), mean error (ME), root mean square error (RMSE), and probability of detection (POD). The capability of GraphCasts' extreme rainfall detection has been further examined with Critical Success Index (CSI) and False Alarm Ratio (FAR) for three threshold benchmarks: 100, 200 and 300 mm. The findings revealed that GraphCast outperforms ECMWF and GFS in routine precipitation forecasting, achieving higher CC (0.57–0.65), lower RMSE (15.66–16.61 mm day^{-1}), and near-perfect POD values (>0.98). It exhibited better performance in central and northern Bangladesh, where monsoon characteristics are more uniform compared to coastal and southeastern hilly regions. However, GraphCast tends to overestimate extreme rainfall events with lower CSI (0.4476–0.5170) and higher FAR (0.4809–0.5519) values. Overall, this study aims to highlight the potential of AI-based operational precipitation forecasting with a path open to integrating hybrid AI-physics frameworks for better extreme event prediction in future.

Keywords: GraphCast, AI, Short Range precipitation forecasting, Extreme Rainfall detection, CSI, FAR

1. Introduction

Accurate short-range precipitation forecasting remains challenging in regions with high spatiotemporal rainfall variability and has significant implications for disaster mitigation, agricultural resilience, and water resource management in flood prone countries like Bangladesh. Though numerical weather prediction (NWP) models have made notable advancements in forecasting, variability led by mesoscale convection, moisture dynamics, and land–atmosphere coupling cannot always be resolved explicitly (1–6). Consequently, global NWP systems like ECMWF and GFS are still having difficulties in tropical rainfall prediction due to parameterization uncertainties, coarse resolution, and initialization errors, particularly in data-sparse observational network (1,2,7,8).

Bangladesh has a monsoon climate, characterized by 80% (typically over 2,000 mm) of its annual precipitation occurring between June and September. The rainfall is strongly influenced by orographic effects, seasonal wind reversals, and large-scale oscillations like ENSO and Indian Ocean Dipole (IOD) (9–12). This inherent variability contributes to an increasing frequency of extreme events, including floods and droughts which disrupts agriculture-dependent livelihoods and impact national GDP(13–17). These socio-economic consequences highlight the necessity of reliable forecasting as erratic rainfall can highly induce food insecurity, disrupted planting cycle and dysfunctional disaster response system. However, limitations in forecast dissemination and public trust are affecting their overall effectiveness (7,18).

The recent progress in AI weather forecasting models is attributed to incorporation of vast reanalysis data and deep learning architectures to achieve skilled predictions without explicit physics and making them complementary to traditional NWP models (19–23). GraphCast, a graph neural network-based (GNN) model, has surpassed the forecasting capability of ECMWF in 90%

of global metrics with 10 days ahead and another AI model namely Pangu-Weather has shown exceptional regional performance across Asia (8,19,20,24–27). While high resolution WRF model provided enhanced local forecast with substantial computational requirements (7,8). But limitations persist in AI based extreme event and local-scale forecasting which stems from biases in rare-event representation, challenges in interpretability, and inconsistencies with physical laws (24–26). Regional evaluations show mixed performance of AI models with reasonable skill in medium range forecasts across East Asia and China while their performance declines in complex seasons like monsoon (27–29). This situation underscores the potential of integrating data-driven and physics-based hybrid models to overcome these gaps (30,31).

The application of AI-based weather forecasting is underexplored in monsoon dominant tropical region against in-situ observations whereas NWP models are staggering with persistent challenges in explaining convective processes (2). Although previous studies have applied machine learning (32,33) or NWP techniques (34,35) to monsoon forecasting in Bangladesh and South Asia, comprehensive evaluation of AI models against NWP utilizing observational data are still scarce limiting insights into their complementary potential. In Bangladesh, emerging studies using limited datasets indicate promising potential but still fall short of the scale and capability of foundation-model-driven systems (26,36,37).

To address this gap, the present study employs GraphCast, a GNN-based model that represents atmospheric states on a multi-resolution mesh, allowing it to capture global-to-local interactions with greater accuracy, speed, and generalization than traditional physics-based models (19). The main objective of this research is to generate 1–3-day precipitation forecast over Bangladesh with 2023 release of GraphCast using BMD observations from 2023–2024, comparing the forecasts with physics-based ECMWF and GFS models and evaluating the operational potential of the model in data-sparse monsoon environments, including extreme event prediction.

2. Data

2.1 Observational Data

Daily cumulative precipitation data were obtained from 43 Bangladesh Meteorological Department (BMD) stations for validating the forecast generated by GraphCast between 2023-24. The data integrity was ensured by exclusion of missing values and adjustments of trace amount. The weather stations are distributed throughout the country to facilitate the regional forecast skill while accounting for topographic and climatic variations (14).

2.2 ERA5 Reanalysis Data

ERA5 reanalysis data from the European Centre for Medium-Range Weather Forecasts (ECMWF) at 0.25° × 0.25° resolution were provided as inputs for the GraphCast simulations (38–41). The selected variables from single and multiple pressure levels have been utilized as the essential constitute to run the operational GraphCast model during 2023–2024 are documented at Table 1 (Copernicus Climate Data Store). They served as the initialization inputs for realistic atmospheric dynamics modelling.

Table 1. ERA5 single- and multi-layer atmospheric variables with corresponding pressure levels used as GraphCast inputs

Single layer atmospheric variables	Multi-layered atmospheric variables	
	Atmospheric variables	Pressure levels (hPa)
2-m temperature (K)	Temperature (K)	1000, 925, 850, 700, 600, 500, 400, 300, 250, 200, 150, 100, 50
10-m u wind component (m/s)	U component of wind (m/s)	
10-m v wind component (m/s)	V component of wind (m/s)	
Mean sea level pressure (Pa)	Specific humidity (kg/kg)	
TOA incident solar radiation (J/m^2)	Geopotential (m^2/s^2)	
Total precipitation (m)	Vertical wind speed (m/s)	

2.3 Numerical Forecast Data

The comparison between GraphCast and physical models were carried out using 1–3 day precipitation forecasts from ECMWF's Integrated Forecasting System and the National Centers for Environmental Prediction's Global Forecast System (GFS), obtained through the THORPEX Interactive Grand Global Ensemble archive. Both models operated at 0.5° × 0.5° resolution for 2023–2024, enabling a consistent assessment of AI versus traditional NWP performance in a monsoon environment (2,27).

3. Methods

3.1 GraphCast Forecasting Framework

The architecture of GraphCast follows an encoder-processor-decoder based-structure that directly uses reanalysis data for forecast generation while avoiding explicit physics equations (19). The encoder maps atmospheric states from latitude-longitude grid onto a multi-resolution icosahedral mesh graph, capturing multi-scale interactions. The processor utilizes multiple GNN layers for message passing between mesh nodes and iteratively keeps updating the model atmospheric dynamics. The decoder then projects these features back to the grids, producing the next state prediction (Fig 1). The operational model, developed by Google DeepMind, is trained on ERA5 data from 1979–2017 and generates 6-hour forecasts autoregressively by ingesting the current state along with the previous 6-hour data. By performing 12 such autoregressive steps, it produces 1–3 day accumulated forecasts at 0.25° resolution, which are then interpolated to station locations using nearest-neighbor mapping, with batch processing enabling efficient high-resolution simulations over complex terrain (20,21).

Fig 1. Schematic overview of the GraphCast model architecture. Showing the encoder embedding grid states onto a multi-mesh graph (a, d), processor updating via message passing (b, e, g), and decoder projecting predictions on the original grid (c, f) [adapted from (19)]

3.2 Evaluation Metrics

Performance was assessed using correlation coefficient (CC) for association, mean error (ME) for bias, root mean square error (RMSE) for deviation, and probability of detection (POD) for event capture, computed over 1-, 2-, and 3-day accumulations (optimal: CC/POD = 1; ME/RMSE = 0):

$$CC = \frac{\frac{1}{N}\sum_{i=1}^{N}\left(F_i - \overline{F}\right)\left(O_i - \overline{O}\right)}{\sigma F \sigma O} \tag{1}$$

$$ME = \frac{1}{N}\sum_{i-1}^{N}(F_i - O_i) \tag{2}$$

$$RMSE = \sqrt{\frac{1}{N}\sum_{i-1}^{N}(F_i - O_i)^2} \tag{3}$$

$$POD = \frac{n_{fo}}{n_{fo} + n_o} \tag{4}$$

Where F_i and O_i denote forecasted and observed values, $\overline{F}$ and $\overline{O}$ are means, σF and σO are standard deviations, n_{fo} is the count of correctly detected events, and n_o is the number of missed observations. N represents the number of data points or samples in the dataset being compared.

For extremes (thresholds: 100, 200, 300 mm), critical success index (CSI; optimal = 1) and false alarm ratio (FAR; optimal = 0) were applied (30,36):

$$CSI = \frac{n_{fo}}{n_{fo} + n_o + n_f} \tag{5}$$

$$FAR = \frac{n_f}{n_{fo} + n_f} \tag{6}$$

Here, n_{fo} is the count of correctly detected events (hits), n_o is the number of missed observations (misses), and n_f is the number of false alarms.

4. Results

4.1 GraphCast Forecast Performance

The spatial distribution of GraphCast's precipitation forecast skill across Bangladesh for 1-3-day lead times during 2023–2024 is depicted in Fig 2. IT demonstrates robust performance, with domain-averaged correlation coefficients (CC) declining from 0.65 at 1 day to 0.57 at 3 days, mean errors (ME) ranging from −0.20 to −0.98 mm day^{-1}, root mean square errors (RMSE) increasing from 15.66 to 16.61 mm day^{-1}, and probability of detection (POD) decreasing from 0.945 to 0.922, indicating gradual skill degradation.

Fig 1. Spatial distribution of GraphCast precipitation forecast performance metrics over Bangladesh for 1-3-day lead times during 2023–2024. Panels depict correlation coefficient (CC: a, e, i), mean error (ME: b, f, j; mm day^{-1}), root mean square error (RMSE: c, g, k; mm day^{-1}), and probability of detection (POD: d, h, l).

Spatially, CC (panels a, e, i) is highest (0.70–0.80) in central and northern regions at 1-day lead, reflecting strong pattern capture in monsoon-influenced areas, but diminishes to 0.65–0.75 at 2 day lead and 0.60–0.70 at 3 day lead, with lower values (0.60–0.70 at 1 day, decreasing further) in southern and eastern zones prone to convective variability. ME (panels b, f, j) shows minimal bias (−4 to +4 mm day^{-1} at 1 day, broadening to −6 to +6 mm day^{-1} at day 3), with slight overestimation in southern stations and underestimation in northern and northeastern zones, consistent across leads. RMSE (panels c, g, k) ranges from 8–35 mm day^{-1} at 1 day, increasing to 10–38 mm day^{-1} at day 2 and 12–40 mm day^{-1} at day 3, with lowest errors in central/northern Bangladesh, highlighting regional skill advantages. POD (panels d, h, l) remains high (0.980–1.000 at 1 day, 0.975–1.000 at day 2, 0.970–1.000 at day 3), demonstrating effective event detection nationwide, though slightly reduced in extremes.

4.2 ECMWF Forecast Performance

The spatial heterogeneity ECMWF's precipitation forecast skill across Bangladesh for 1–3-day lead times during 2023–2024 is demonstrated in Fig 3, based on validation against BMD station observations. Overall, ECMWF exhibits moderate performance, with correlation coefficients (CC) ranging from 0.18–0.60, mean errors (ME) between −3.9 and +4.6 mm day^{-1}, root mean square errors (RMSE) from 12–35 mm day^{-1}, and probability of detection (POD) of 0.92–1.00, reflecting gradual degradation with longer leads.

Fig 2. Spatial distribution of ECMWF precipitation forecast performance metrics over Bangladesh for 1-3-day lead times during 2023–2024. Panels depict correlation coefficient (CC: a, e, i), mean error (ME: b, f, j; mm day-1), root mean square error (RMSE: c, g, k; mm day^{-1}), and probability of detection (POD: d, h, l).

Spatially, CC (panels a, e, i) ranges from 0.18–0.55 at day 1 (higher in northern/northeastern regions, lower in southeast/southern coastal areas), 0.20–0.56 at day 2 (moderately higher in central/southern parts, lower in northern/southeastern coastal zones), and 0.22–0.60 at day 3 (generally lower, particularly in southern/coastal areas). ME (panels b, f, j) shows values of −3.7 to +4.0 mm day^{-1} at 1 day (slight positive biases in northwestern/southern areas, negative in southeastern/coastal regions), broadening to −3.6 to +4.6 mm day^{-1} at 2 day (similar patterns) and −3.9 to +4.3 mm day^{-1} at 3 day (stronger negatives in northeastern/southern regions). RMSE (panels c, g, k) varies from 12–34 mm day^{-1} at 1 day (smaller in central/western areas, larger in northeast), extending to 13–34 mm day^{-1} at day 2 (lowest in central/western, higher in northeast/southeastern coast), with comparable ranges at day 3. POD (panels d, h, l) remains high at 0.95–1.00 for day 1, 0.92–0.99 for day 2, and consistently elevated at day 3, indicating reliable event detection nationwide.

4.3 GFS Forecast Performance

Fig 4 illustrates the spatial distribution of GFS's precipitation forecast skill across Bangladesh for 1–3-day lead times during 2023–2024, based on validation against BMD station observations. Overall, GFS displays moderate performance, with domain-averaged correlation coefficients (CC) declining from 0.40 at 1 day to 0.33 at day 3, mean errors (ME) ranging from −1.10 to −1.52 mm day^{-1} indicating underestimation, root mean square errors (RMSE) increasing from 18.61 to 19.31 mm day^{-1}, and probability of detection (POD) decreasing from 0.919 to 0.900.

Fig 3. Spatial distribution of GFS precipitation forecast performance metrics over Bangladesh for 1-3-day lead times during 2023–2024. Panels depict correlation coefficient (CC: a, e, i), mean error (ME: b, f, j; mm day^{-1}), root mean square error (RMSE: c, g, k; mm day^{-1}), and probability of detection (POD: d, h, l).

Spatially, CC (panels a, e, i) ranges from 0.15–0.55 at day 1 (higher in northern/northeastern regions, lower in southeast/southern coastal areas), 0.18–0.53 at day 2 (moderately higher in central/southern parts, lower in northern/southeastern coastal zones), and 0.20–0.50 at day 3 (generally lower, particularly in southern/coastal areas). ME (panels b, f, j) shows values of −3.8 to +4.2 mm day^{-1} at day 1 (positive biases in northwestern/southern areas, negative in southeastern/coastal regions), broadening to −3.7 to +4.5 mm day^{-1} day 2 (similar patterns) and −4.0 to +4.1 mm day^{-1} at day 3 (stronger negatives in northeastern/southern regions). RMSE (panels c, g, k) varies from 12–35 mm day^{-1} at day 1(smaller in central/western areas, larger in northeast), extending to 13–36 mm day^{-1} at day 2 (lowest in central/western, higher in northeast/southeastern coast), and similar ranges at day 3. POD (panels d, h, l) remains robust, with 0.90–1.00 at day 1, 0.88–0.99 at day 2, and 0.85–0.98 at day 3, indicating effective event detection despite biases.

4.4 GraphCast Performance in Monsoon Season

Fig 5 displays the spatial distribution of mean error (ME) and root mean square error (RMSE) for GraphCast precipitation forecasts during the monsoon season (June–September) over Bangladesh at 1-, 2-, and 3-day lead times, validated against BMD station observations from 2023–2024.

Fig 5. Spatial distribution of GraphCast precipitation forecast performance metrics over Bangladesh for 1–3-day lead times during 2023–2024. Panels show mean error (ME: a, c, e; mm day^{-1}) and root mean square error (RMSE: b, d, f; mm day^{-1}) for 1-day (a, b), 2-day (c, d), and 3-day (e, f) forecasts.

For the 1-day lead (panels a, b), ME ranges from -11.56 to 10.49 mm, showing predominant negative values (underestimation) in northern and central regions, with positive values (overestimation) in southern coastal areas; RMSE ranges from 10.76 to 48.02 mm, with most stations falling between 15.52 and 25.10 mm, and higher errors in northeastern and southeastern stations. For the 2-day lead (panels c, d), ME ranges from -10.28 to 13.80 mm, maintaining similar spatial patterns of underestimation in the north/center and overestimation in the south; RMSE ranges from 11.81 to 41.19 mm, with most stations falling between 16.16 and 26.42 mm, and elevated errors in the northeast. For the 3-day lead (panels e, f), ME ranges from -7.99 to 16.58 mm, exhibiting increased overestimation in southern zones; RMSE ranges from 12.22 to 41.83 mm, with most stations falling between 16.86 and 26.77 mm, and higher deviations in northeastern and some central stations.

4.5 Comparative Model Performance

Fig 6 presents domain-averaged metrics for cumulative precipitation forecasts by GraphCast, ECMWF, and GFS across 1- to 3-day lead times during 2023–2024.

Fig 6. Domain-averaged performance metrics for precipitation forecasts over Bangladesh for 1–3-day lead times during 2023–2024. Panels show correlation coefficient (CC), mean error (ME; mm day^{-1}), root mean square error (RMSE; mm day^{-1}), and probability of detection (POD) for GraphCast (blue), ECMWF (orange), and GFS (green).

GraphCast outperforms in CC (0.63–0.57), RMSE (15.8–16.5 mm day⁻¹), and POD (0.99–0.98), with minimal degradation, reflecting superior pattern capture and event detection. ECMWF shows moderate CC (0.41–0.39) and RMSE (18.2–18.7 mm day⁻¹), with lower POD (0.98–0.96). GFS exhibits comparable CC (0.40–0.35) but higher RMSE (18.5–19.0 mm day⁻¹) and POD (0.92–0.90). All models display negative ME (−0.3 to −1.4 mm day⁻¹), indicating underestimation, with GraphCast and GFS more pronounced.

4.6 Performance for Extreme Rainfall Events

The critical success index (CSI) and false alarm ratio (FAR) for GraphCast, ECMWF, and GFS at extreme rainfall thresholds of 100, 200, and 300 mm across 1-, 2-, and 3-day lead times are summarized in Table 2. These metrics evaluate the models' skill in detecting high-intensity events.

Table 2. Critical Success Index (CSI) and False Alarm Ratio (FAR) for GraphCast, ECMWF, and GFS at extreme rainfall thresholds and lead times.

Threshold(mm)		**100**		**200**		**300**	
Model	**Lead_Time**	**CSI**	**FAR**	**CSI**	**FAR**	**CSI**	**FAR**
ECMWF	**1day**	0.4876	0.4969	0.5012	0.4779	0.5092	0.4654
	2day	0.4936	0.4867	0.5059	0.4677	0.5129	0.4561
	3day	0.4878	0.4911	0.5002	0.4731	0.507	0.4614
GraphCast	**1day**	0.4603	0.5393	0.4949	0.5041	0.517	0.4809
	2day	0.4582	0.5415	0.4864	0.5125	0.5042	0.494
	3day	0.4476	0.5519	0.4722	0.5267	0.4902	0.508
GFS	**1day**	0.5121	0.4556	0.5162	0.4477	0.5212	0.4364
	2day	0.5202	0.4419	0.5227	0.4313	0.5251	0.4212
	3day	0.5144	0.4474	0.5182	0.4346	0.5201	0.4264

At the 100 mm threshold, CSI ranges from 0.4476 to 0.5202, with GFS highest (0.5121–0.5202) and GraphCast lowest (0.4476–0.4603); FAR varies from 0.4419 to 0.5519, with GFS lowest (0.4419–0.4556) and GraphCast highest (0.5393–0.5519). For 200 mm, CSI spans 0.4722–0.5227, with GFS leading (0.5162–0.5227) and GraphCast trailing (0.4722–0.4949); FAR ranges 0.4313–

0.5267. At 300 mm, CSI is 0.4902–0.5251, with GFS superior (0.5201–0.5251) and GraphCast lower (0.4902–0.5170); FAR is 0.4212–0.5080.

CSI modestly increases and FAR decreases with higher thresholds across models, indicating better relative skill for rarer events (Nevo et al., 2022). GFS outperforms with highest CSI and lowest FAR, followed by ECMWF (CSI: 0.4876–0.5129; FAR: 0.4561–0.4969), while GraphCast shows lower CSI and higher FAR, suggesting overprediction of extremes due to underrepresented rare events in training data (24,26).

4. Discussion

The AI driven GNN structure of GraphCast captures broad atmospheric patterns and non-linear dynamics associated with rainfall variability efficiently compared to ECMWF and GFS (19–21) as reflected in higher CC (0.57–0.65) and lower RMSE (15.66–16.61 mm day^{-1}) across 1- to 3-day leads over Bangladesh in domain average metrics for short-range forecasting. Among the models ECMWF showed the smallest bias (−0.23 to −0.43 mm day^{-1}), followed by GraphCast with moderate bias (−0.20 to −0.98 mm day^{-1}), while GFS exhibited the strongest underestimation (−1.10 to −1.52 mm day^{-1}). In monsoon-prone regions where small rainfall can trigger flooding (7,30), the near perfect POD values (≈0.999) ensure GraphCast's reliability in rainfall detection and better representation of monsoon precipitation variability. However, the inherent unpredictability of Bangladesh's convective tropical climate (6,10) causes all three models to lose skill with increasing lead time, with GraphCast showing a slightly larger rise in RMSE due to accumulated autoregressive uncertainty.

The current study has found relatively better performance of GraphCast in central and northern Bangladesh along with higher CC and lower RMSE values which indicated improved simulation of monsoon dynamics over relatively uniform terrain. On the contrast, southeastern regions observed reduced skill in forecasting which may correspond to findings from similar evaluation studies carried over monsoon-dominated complex topography where AI models capture large-scale circulation and moisture transport effectively but face challenges with highly localized extreme events (5,29,42). As GraphCast is trained on ERA5 reanalysis data, it has better data assimilation which can capture regional heterogeneity better than traditional physics-based models that face difficulties in explaining sub-grid scale orographic and convective processes, making it suitable for short-term water management and agricultural planning where rainfall variability strongly affects food security (3,4,12,13)

The monsoon performance of GraphCast is relatively weak over Bangladesh with underestimation in northern/central areas and overestimation in the south while RMSE values are higher than annual averages, indicating model's sensitivity to convective variability and orographic effects during peak monsoon periods (5,6), though its near-perfect POD still supports strong flood-warning capability. Alongside monsoon forecasting, GraphCast also underperforms compared to GFS and ECMWF in extreme rainfall event (100–300 mm) detection, exhibiting higher FAR and lower CSI, likely due to rare-event biases from reanalysis-based training lacking high-magnitude rainfall events weather samples in historical data (24–26). GFS performs best at these thresholds as GFS's ensemble assimilation methods allow better representation of outliers (2,27). Higher CSI means the model is correctly capturing more real rainfall events, while lower FAR means it is issuing fewer false alarms—together indicating more accurate and reliable heavy-rain predictions. The observed increase in CSI and corresponding decrease in FAR with higher magnitude thresholds across models suggests improved relative accuracy for rarer events, as false detections decline with increasing rainfall magnitude (30).

Finally, the findings of the study suggests that GraphCast outperformed ECMWF in 1–3-day precipitation forecasts in Bangladesh with RMSE values ranging between 9.08–18.66 mm day^{-1}. Similar outputs were found over China from GraphCast forecast where RMSE has fallen between 0.44–9.38 mm day^{-1}. This difference reflects Bangladesh's highly variable monsoon rainfall with extreme convective and orographic effects (5,6), compared to China's more stable temperate precipitation patterns (28). These conditions imply that GraphCast holds substantial potential for operational short-range forecasting in Bangladesh, particularly for routine precipitation prediction and flood early warning. However, optimization for extreme event forecasting remains necessary. Future improvements could address forecast uncertainty by integrating ensemble or probabilistic extensions (22) or hybrid frameworks combining AI and physics-based models (26).

5. Conclusion

This study demonstrates that GraphCast outperforms ECMWF and GFS in 1–3-day precipitation forecasts over Bangladesh, with higher correlations, lower errors, and near-perfect detection rates. Forecast skill declines with lead time for all models, but GraphCast remains robust for near-term operational use. The model tends to overpredict extreme rainfall (100–300 mm), resulting in higher false alarms compared to GFS. Overall, GraphCast demonstrates substantial promise for improving short-term precipitation forecasts in tropical environments like Bangladesh and integrating it with traditional physics-based models may offer a more balanced approach to capturing both typical and extreme rainfall events. The current study can be further extended in future with longer datasets and satellite-based observations to assess interannual consistency and enhance generalizability.

Acknowledgement

The authors gratefully acknowledge the Google TPU Research Cloud (TRC) program for providing complimentary access to Cloud TPU resources, which enabled the computational experiments and large-scale GraphCast simulations conducted in this study. Access to multiple TPU generations substantially supported the high-performance processing required for this work.

The authors also acknowledge the Bangladesh Meteorological Department (BMD) for providing observational precipitation data, and the Copernicus Climate Data Store for access to ERA5 reanalysis inputs used to drive the GraphCast model. Their data contributions were essential for the evaluation and validation of the forecasts.

Finally, the authors thank the Department of Meteorology, University of Dhaka, for continuous academic guidance and institutional support throughout the duration of this research.

Data availability

All raw data is available from the authors upon reasonable request.

CRediT authorship contribution statement

Munad Hasan: Conceptualization, Data curation, Formal analysis, Methodology, Codes, Visualization, Validation, Writing – original draft **Shabista Yildiz:** Methodology, Analysis, Visualization, Supervision, Writing– review and editing; **Mohammad Kamruzzaman:** Analysis, Writing – review and editing

Declaration of Competing Interest

The authors declare that they have no known competing financial interests or personal relationships that could have appeared to influence the work reported in this paper.

References

1. Aggarwal R, Kumar R. A Comprehensive Review of Numerical Weather Prediction Models. Int J Comput Appl. 2013 Jul 26;74(18):44–8.
2. Brotzge JA, Berchoff D, Carlis DL, Carr FH, Carr RH, Gerth JJ, et al. Challenges and Opportunities in Numerical Weather Prediction. Bull Am Meteorol Soc. 2023 Mar;104:E698–705.
3. Uddin SMN, Pramanik MdSK, Hossen MdS. Impact of Temperature and Rainfall on Agricultural Production in the Southern Part of Bangladesh. Malaysian Journal of Business, Economics and Management. 2024 Oct;196–201.
4. Ahmed MR. Climate shocks' impact on agricultural income and household food security in Bangladesh: An implication of the food insecurity experience scale. Heliyon. 2024 Feb;10.
5. Endo N, Matsumoto J, Hayashi T, Terao T, Murata F, Kiguchi M, et al. Trends in precipitation characteristics in Bangladesh from 1950 to 2008. Scientific Online Letters on the Atmosphere. 2015;11:113–7.
6. Rafiuddin M, Uyeda H, Islam MN. Regional and seasonal variations of precipitation systems in Bangladesh. Sri Lankan Journal of Physics. 2012 Feb;12:7.
7. Singhal A, Raman A, Jha SK. Potential Use of Extreme Rainfall Forecast and Socio-Economic Data for Impact-Based Forecasting at the District Level in Northern India. Front Earth Sci (Lausanne). 2022 May;10.
8. Xu H, Zhao Y, Zhao D, Duan Y, Xu X. Improvement of disastrous extreme precipitation forecasting in North China by Pangu-weather AI-driven regional WRF model. Environmental Research Letters. 2024 May 1;19(5).
9. Ahmed R, Kim IK. Patterns of Daily Rainfall in Bangladesh During the Summer Monsoon Season: Case Studies at Three Stations. Phys Geogr. 2003;24:295–318.
10. Alam E, Hridoy AEE, Tusher SMSH, Islam ARMT, Islam MK. Climate change in Bangladesh: Temperature and rainfall climatology of Bangladesh for 1949-2013 and its implication on rice yield. PLoS One. 2023 Oct;18.
11. Das LC, Zhang Z, James M, Crabbe C, Liu A. Spatio-temporal patterns of rainfall variability in Bangladesh. International Journal of Global Warming. 2024;33:206–21.
12. Rahman MN, Azim SA. Spatiotemporal evaluation of rainfall trend during 1979-2019 in seven climatic zones of Bangladesh. Geology, Ecology, and Landscapes. 2023;7:340–55.
13. Ahmed S, Islam T, Haque A, Bhandari H. https://cgspace.cgiar.org/items/203a67b2-fb77-4ffc-b7be-c23a65fafdd4. 2024. Effect of rainfall variability on cropping windows of Patuakhali and Rangpur Regions.
14. Kumar U, Werners S, Roy S, Ashraf S, Hoang LP, Datta DK, et al. Role of information in farmers' response toweather and water related stresses in the lower Bengal Delta, Bangladesh. Sustainability (Switzerland). 2020 Aug;12.

15. Hassan SMQ, Mallik MAK, Akhter MAE, Chowdhury MAM. TREND ANALYSIS AND SPATIAL DISTRIBUTION OF MONSOON PRECIPITATION OVER BANGLADESH DURING 1951-2012. Vol. 06, Journal of Engineering Science. 2015.

16. Hossain MF. Impact of Climate Change in Bangladesh: Rainfall. Vol. 2, International Journal of Agriculture Innovations and Research. 2002.

17. Mishu RA, Mallick J, Akter MY, Fattah MA, Kamruzzaman M, Salam MA, et al. Spatial and temporal variability of future extreme precipitation in Bangladesh using CMIP6 models. Journal of Water and Climate Change. 2025 Apr;16:1281–309.

18. Chapagain PS, Shrestha S, Islam MN, Rai SC, Zhang Y, Yan J, et al. Weather information sources, sharing platforms, and trustworthiness for climate change adaptation in Bangladesh, India, and Nepal. Clim Dev. 2025;

19. Lam R, Sanchez-Gonzalez A, Willson M, Wirnsberger P, Fortunato M, Alet F, et al. Learning skillful medium-range global weather forecasting. Science (1979). 2023 Dec;382:1416–22.

20. Bi K, Xie L, Zhang H, Chen X, Gu X, Tian Q. Accurate medium-range global weather forecasting with 3D neural networks. Nature. 2023 Jul;619:533–8.

21. Pathak J, Subramanian S, Harrington P, Raja S, Chattopadhyay A, Mardani M, et al. FourCastNet: A Global Data-driven High-resolution Weather Model using Adaptive Fourier Neural Operators. 2022 Feb;

22. Price I, Sanchez-Gonzalez A, Alet F, Andersson TR, El-Kadi A, Masters D, et al. Probabilistic weather forecasting with machine learning. Nature. 2025 Jan 2;637(8044):84–90.

23. Zhong X, Chen L, Liu J, Lin C, Qi Y, Li H. FuXi-Extreme: Improving extreme rainfall and wind forecasts with diffusion model. Sci China Earth Sci. 2024 Dec;67:3696–708.

24. Sun YQ, Hassanzadeh P, Zand M, Chattopadhyay A, Weare J, Abbot DS. Can AI weather models predict out-of-distribution gray swan tropical cyclones? Proc Natl Acad Sci U S A. 2025 May;122.

25. Zhang Z, Fischer E, Zscheischler J, Engelke S. Numerical models outperform AI weather forecasts of record-breaking extremes. 2025 Aug;

26. Bodnar C, Bruinsma WP, Lucic A, Stanley M, Allen A, Brandstetter J, et al. A foundation model for the Earth system. Nature. 2025 May 29;641(8065):1180–7.

27. Liu CC, Hsu K, Peng MS, Chen DS, Chang PL, Hsiao LF, et al. Evaluation of five global AI models for predicting weather in Eastern Asia and Western Pacific. NPJ Clim Atmos Sci. 2024 Dec 1;7(1).

28. Yan Z, Lu X, Wu L, Liu F, Qiu R, Cui Y, et al. Evaluation of precipitation forecasting base on GraphCast over mainland China. Sci Rep. 2025 Dec 1;15(1).

29. Gupta A, Sheshadri A, Suri D. MAUSAM: An Observations-focused assessment of Global AI Weather Prediction Models During the South Asian Monsoon. 2025 Sep;

30. Nevo S, Morin E, Gerzi Rosenthal A, Metzger A, Barshai C, Weitzner D, et al. Flood forecasting with machine learning models in an operational framework. Hydrol Earth Syst Sci. 2022 Aug;26:4013–32.

31. Portuguez-maurtua M, Arumi JL, Lagos O, Stehr A, Arquiñigo NM. Filling Gaps in Daily Precipitation Series Using Regression and Machine Learning in Inter-Andean Watersheds. Water (Switzerland). 2022 Jun;14.

32. Billah M, Adnan MN, Akhond MR, Ema RR, Hossain MA, Md. Galib S. Rainfall prediction system for Bangladesh using long short-term memory. Open Computer Science. 2022 Jan;12:323–31.

33. Osmani SA, Kim JS, Jun C, Sumon MW, Baik J, Lee J. Prediction of monthly dry days with machine learning algorithms: a case study in Northern Bangladesh. Sci Rep. 2022 Dec;12.

34. Sikder S, Hossain F. Assessment of the weather research and forecasting model generalized parameterization schemes for advancement of precipitation forecasting in monsoon-driven river basins. J Adv Model Earth Syst. 2016 Sep;8:1210–28.

35. Mannan MA, Chowdhury MAM, Karmakar S. Application of NWP model in prediction of heavy rainfall in Bangladesh. In: Procedia Engineering. Elsevier Ltd; 2013. p. 667–75.

36. Islam MA, Shampa MTA. Precipitation prediction in Bangladesh using machine learning approaches. International Journal of Hydrology Science and Technology. 2024;18:23–56.

37. Wu Y, Yang J, Zhang Z, Das LC, Crabbe MJC. High-Resolution Temperature Evolution Maps of Bangladesh via Data-Driven Learning. Atmosphere (Basel). 2024 Mar;15.

38. Assamnew AD, Mengistu Tsidu G. Assessing improvement in the fifth-generation ECMWF atmospheric reanalysis precipitation over East Africa. International Journal of Climatology. 2023 Jan;43:17–37.

39. Du M, Huang K, Zhang S, Huang C, Gong Y, Yi F. Water vapor anomaly over the tropical western Pacific in El Niño winters from radiosonde and satellite observations and ERA5 reanalysis data. Atmos Chem Phys. 2021 Sep;21:13553–69.

40. Huang H, Huang Y. Radiative sensitivity quantified by a new set of radiation flux kernels based on the ECMWF Reanalysis v5 (ERA5). Earth Syst Sci Data. 2023 Jul;15:3001–21.

41. Patra A, Min SK, Seong MG. Climate Variability Impacts on Global Extreme Wave Heights: Seasonal Assessment Using Satellite Data and ERA5 Reanalysis. J Geophys Res Oceans. 2020 Dec;125.

42. Choudhury A, Panda J. Development of a Data-driven weather forecasting system over India with Pangu-Weather architecture and IMDAA reanalysis Data. 2025 Mar 17; Available from: http://arxiv.org/abs/2503.12956

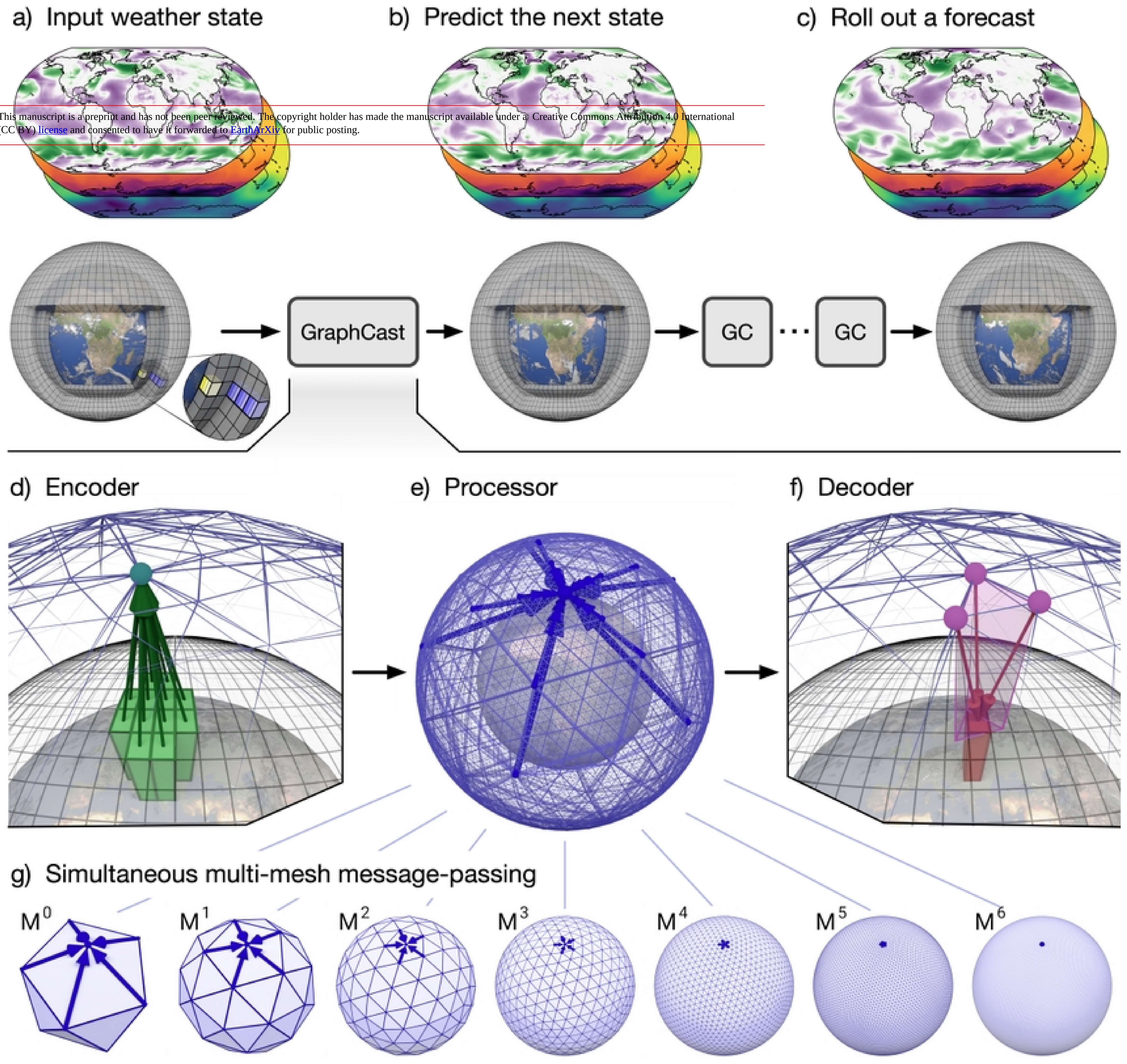

a) Input weather state
b) Predict the next state
c) Roll out a forecast
GraphCast
GC
GC
d) Encoder
e) Processor
f) Decoder
g) Simultaneous multi-mesh message-passing
M^0
M^1
M^2
M^3
M^4
M^5
M^6

Figure

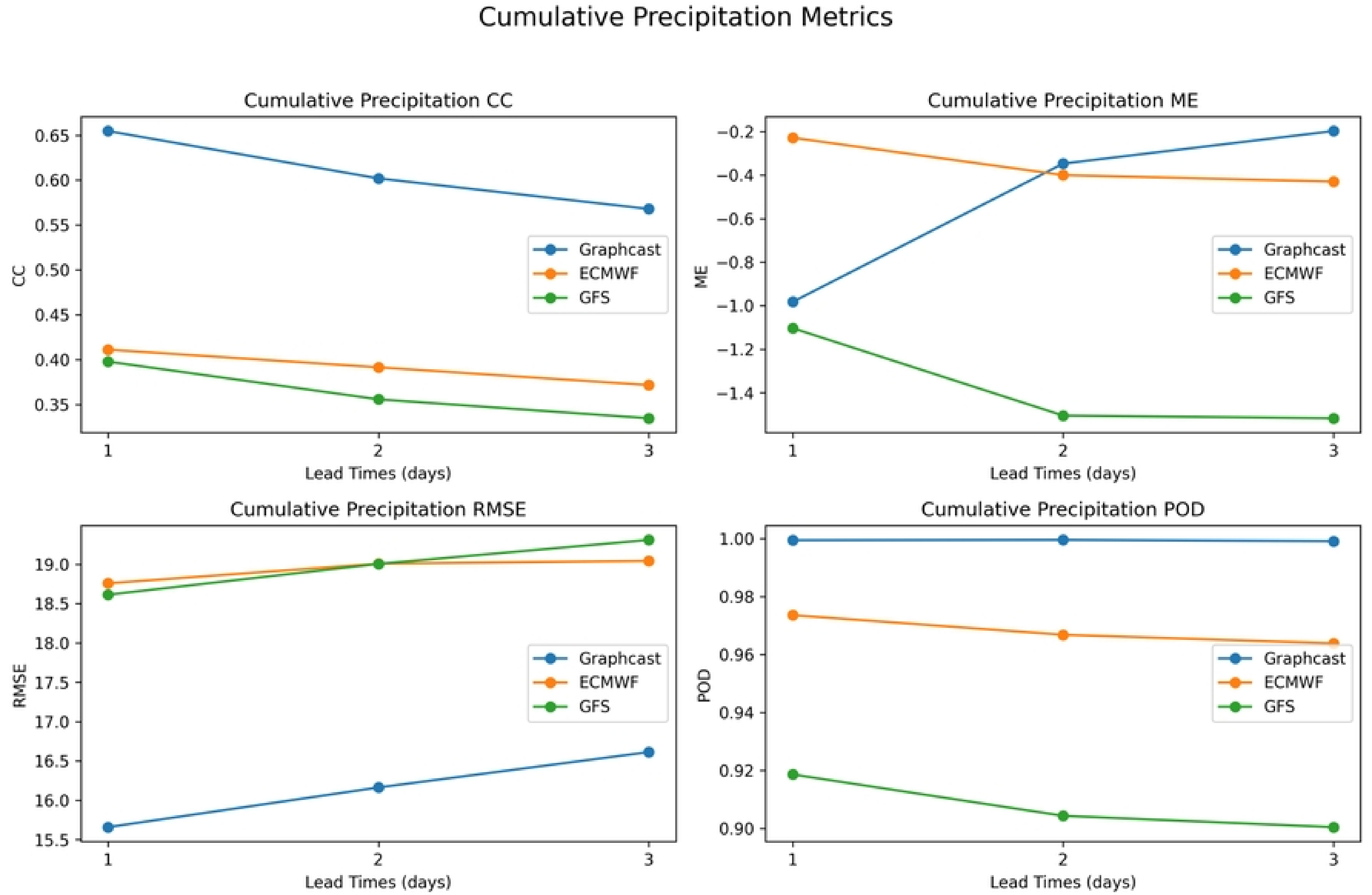

Cumulative Precipitation Metrics
Cumulative Precipitation CC
Cumulative Precipitation ME
Cumulative Precipitation RMSE
Cumulative Precipitation POD
CC
ME
RMSE
POD
Lead Times (days)
Graphcast
ECMWF
GFS

Figure

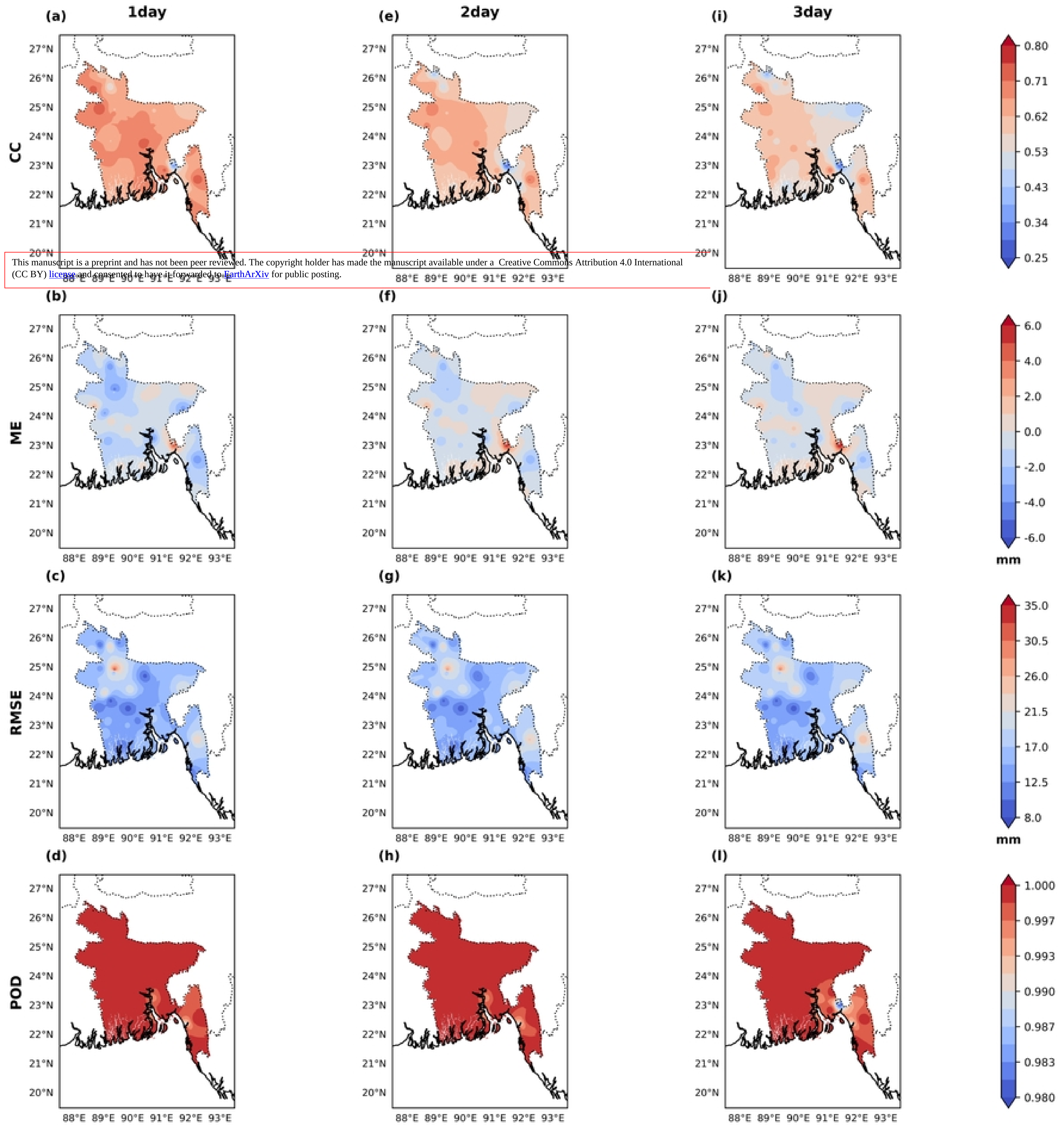

(a)
1day
(e)
2day
(i)
3day
(b)
(f)
(j)
(c)
(g)
(k)
(d)
(h)
(l)
CC
ME
RMSE
POD
27°N
26°N
25°N
24°N
23°N
22°N
21°N
20°N
88°E 89°E 90°E 91°E 92°E 93°E
0.80
0.71
0.62
0.53
0.43
0.34
0.25
6.0
4.0
2.0
0.0
-2.0
-4.0
-6.0
mm
35.0
30.5
26.0
21.5
17.0
12.5
8.0
mm
1.000
0.997
0.993
0.990
0.987
0.983
0.980

Figure

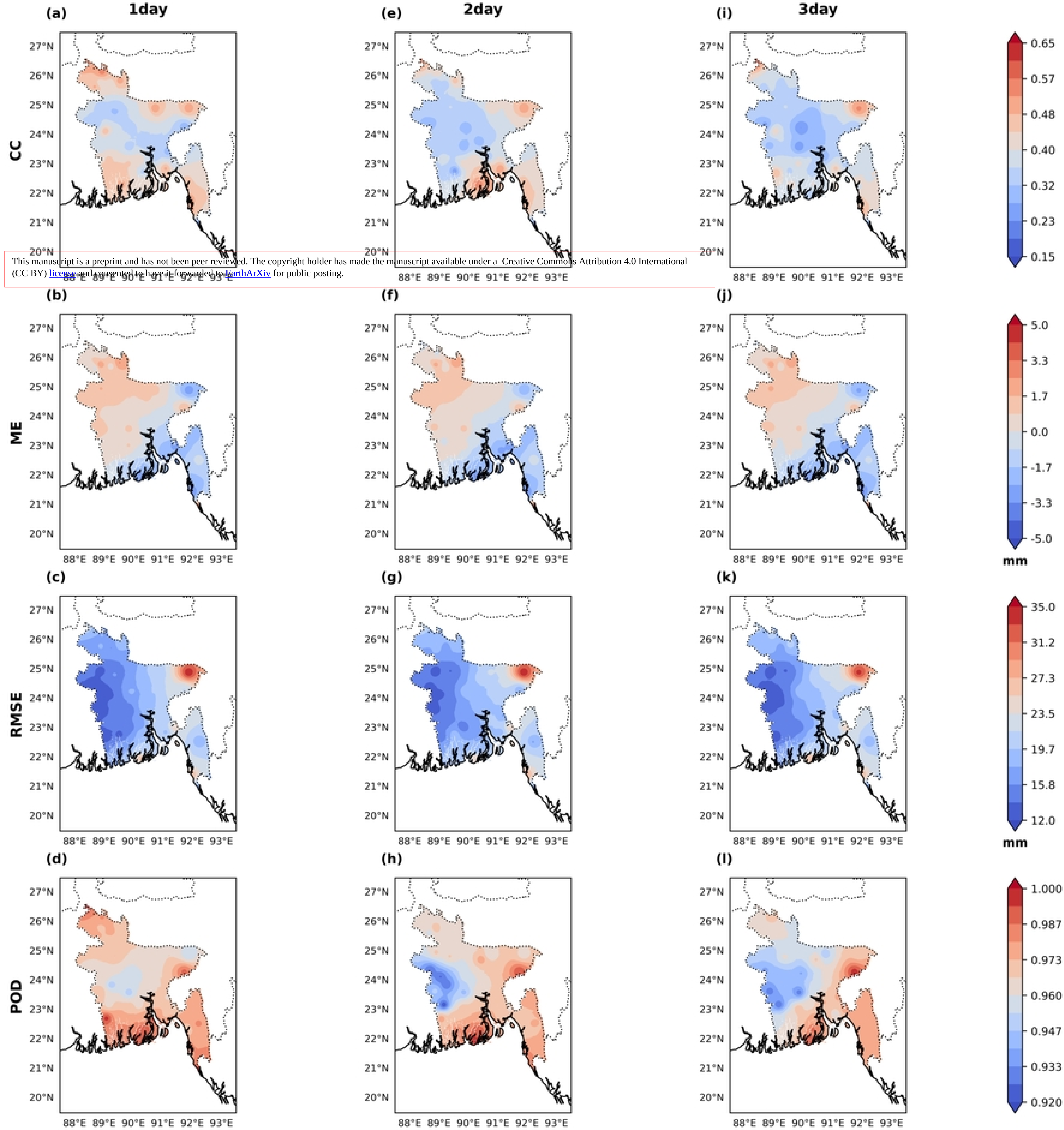
(a)
1day
(e)
2day
(i)
3day
(b)
(f)
(j)
(c)
(g)
(k)
(d)
(h)
(l)
CC
ME
RMSE
POD
27°N
26°N
25°N
24°N
23°N
22°N
21°N
20°N
88°E 89°E 90°E 91°E 92°E 93°E
0.65
0.57
0.48
0.40
0.32
0.23
0.15
5.0
3.3
1.7
0.0
-1.7
-3.3
-5.0
mm
35.0
31.2
27.3
23.5
19.7
15.8
12.0
mm
1.000
0.987
0.973
0.960
0.947
0.933
0.920

Figure

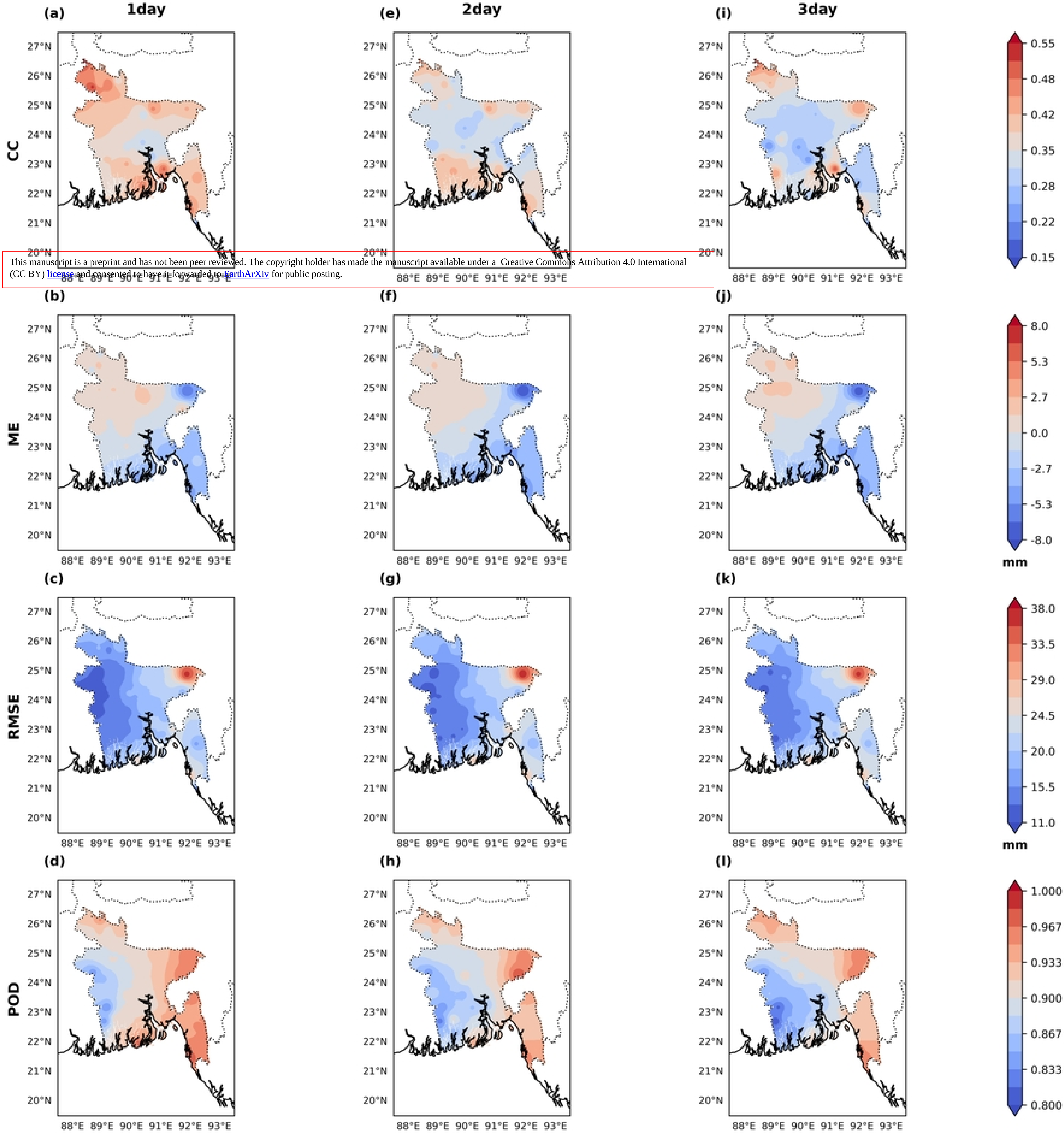
(a)
1day
(e)
2day
(i)
3day
CC
ME
RMSE
POD
(b)
(f)
(j)
(c)
(g)
(k)
(d)
(h)
(l)
27°N
26°N
25°N
24°N
23°N
22°N
21°N
20°N
88°E 89°E 90°E 91°E 92°E 93°E
0.55
0.48
0.42
0.35
0.28
0.22
0.15
8.0
5.3
2.7
0.0
-2.7
-5.3
-8.0
mm
38.0
33.5
29.0
24.5
20.0
15.5
11.0
mm
1.000
0.967
0.933
0.900
0.867
0.833
0.800

Figure

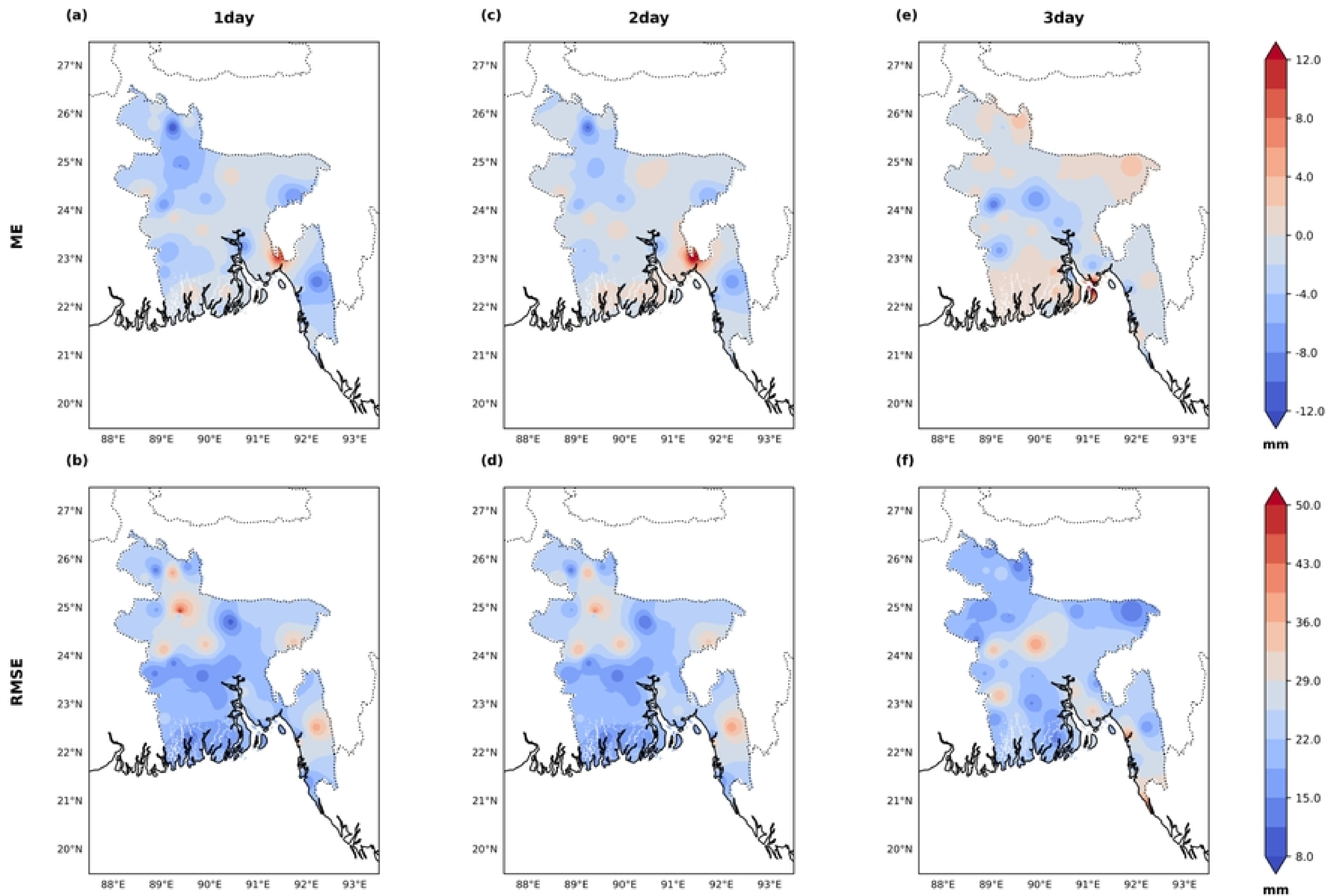
(a)
1day
(c)
2day
(e)
3day
ME
RMSE
(b)
(d)
(f)
27°N
26°N
25°N
24°N
23°N
22°N
21°N
20°N
88°E
89°E
90°E
91°E
92°E
93°E
12.0
8.0
4.0
0.0
-4.0
-8.0
-12.0
mm
50.0
43.0
36.0
29.0
22.0
15.0
8.0
mm

Figure